ANTIOXIDANTS & REDOX SIGNALING
Volume 15, Number 4, 2011

DOI: 10.1089/ars.2010.3767

ORIGINAL RESEARCH COMMUNICATION

RGSZ2 Binds to the Neural Nitric Oxide Synthase PDZ Domain to Regulate Mu-Opioid Receptor-Mediated Potentiation of the *N*-Methyl-D-Aspartate Receptor-Calmodulin-Dependent Protein Kinase II Pathway

Javier Garzón,[1,2] María Rodríguez-Muñoz,[2] Ana Vicente-Sánchez,[1] Concha Bailón,[1,2] Ricardo Martínez-Murillo,[1,3] and Pilar Sánchez-Blázquez[1,2]

Abstract

Morphine increases the production of nitric oxide (NO) *via* the phosphoinositide 3-kinase/Akt/neural nitric oxide synthase (nNOS) pathway. Subsequently, NO enhances *N*-methyl-D-aspartate receptor (NMDAR)/calmodulin-dependent protein kinase II (CaMKII) cascade, diminishing the strength of morphine-activated Mu-opioid receptor (MOR) signaling. During this process, NO signaling is restricted by the association of nNOS to the MOR. ***Aims:*** Here, we examined how nNOS/NO signaling is downregulated by the morphine-activated MOR and how this regulation affects antinociception. ***Results:*** Accordingly, we show that the MOR-NMDAR regulatory loop relies on the negative control of nNOS activity exerted by RGSZ2, a protein physically coupled to the MOR. This regulation requires binding of the nNOS N terminal PDZ domain to the RGSZ2 PDZ binding motifs that lie upstream of the RGS box. ***Innovation:*** Indeed, in RGSZ2-deficient mice morphine over-stimulates the nNOS/NO/NMDAR/CaMKII pathway, causing analgesic tolerance to develop rapidly. Recovery of RGSZ2 levels or inhibition of nNOS, protein kinase C, NMDAR, or CaMKII function restores MOR signaling and morphine recovers its full analgesic potency. ***Conclusion:*** This RGSZ2-dependent regulation of NMDAR activity is relevant to persistent pain disorders associated with heightened NMDAR-mediated glutamate responses and the reduced antinociceptive capacity of opioids. *Antioxid. Redox Signal.* 15, 873–887.

Introduction

Immunohistochemical studies have provided convincing evidence for the colocalization of the Mu-opioid receptor (MOR) and the glutamate-driven *N*-methyl-D-aspartate receptor (NMDAR) in many regions of brain, as well as in the dorsal horn of the spinal cord [reviewed in Garzón *et al*. (16)]. Notably, at the ultrastructural level both receptors frequently colocalize at postsynaptic sites in neurons within these central nervous system regions (9, 17). The midbrain periaqueductal gray (PAG) matter-rostral ventromedial medulla system is involved in the antinociceptive effects of intracerebroventricularly (icv)-injected opioids (28, 47). The PAG is densely innervated by glutamatergic projections from the forebrain, and there is robust colocalization of MOR-NMDAR in the dendrites and somata of ventrolateral PAG neurons (9). This spatial coincidence provides a biological substrate to explain the relationship between the MOR and NMDAR in the supraspinal control of pain perception, as well as accounting for the development of morphine analgesic tolerance due to the MOR-mediated sustained potentiation of NMDAR calcium currents (8, 23). Indeed, events initiated *via* NMDARs support the phosphorylation of morphine-activated MORs in the plasma membrane, but without forcing their internalization and ensuing uncoupling from regulated transduction (29, 35, 39, 46).

A series of G protein-coupled receptors (GPCRs) activate protein kinase C (PKC) and Src to enhance NMDAR-regulated calcium currents (21, 30). The MOR to regulate NMDAR activity requires PKC, Src, and other signaling proteins as well (36, 38). One of these proteins, the histidine triad nucleotide binding protein 1 (HINT1), binds to the MOR C terminus (CT) and to the Rz subfamily of regulators of G protein signaling, RGSZ1 and RGSZ2 (2, 18, 37). Upon activation of MOR, this HINT1-RGSZ complex recruits other proteins to the MOR environment, such as the inactive form

[1]Cajal Institute, Consejo Superior de Investigaciones Científicas, Madrid, Spain.
[2]CIBER of Mental Health (CIBERSAM), Instituto de Salud Carlos III, Madrid, Spain.
[3]Red Neurovascular (RENEVAS), Instituto de Salud Carlos III, Madrid, Spain.

Innovation

Pharmacological, electrophysiological, and behavioral studies have demonstrated a relevant role of the glutamate-binding *N*-methyl-D-aspartate receptor (NMDAR) in the genesis and/or maintenance of chronic/persistent pain states. In these conditions, mu-opioid receptor (MOR)-activating opioids do not provide efficacious relief and this complicates their clinical use to treat persistent neuropathic pain. The relationship between MORs and NMDARs is bidirectional, and tolerance to morphine develops as a consequence of MOR-induced potentiation of NMDAR activity via nitric oxide (NO)-mediated release of zinc, zinc-mediated recruitment of PKCγ, and the subsequent PKC-mediated activation of Src. Our study shows that morphine regulates neural nitric oxide synthase (nNOS) by a push–pull mechanism. It promotes nNOS activation via the MOR/phosphoinositide 3-kinase (PI3K)/Akt pathway and it also diminishes NO production, fomenting the protecting association of nNOS with the MOR apart from the activating effects of Akt. This regulation requires binding of the nNOS N-terminal PDZ domain to the regulator of G protein signaling Z2 (RGSZ2) PDZ binding motifs that lie upstream of the RGS box. The MOR bears the histidine triad nucleotide binding protein 1 (HINT1)-RGSZ2 complex in its C-terminus, where nNOS-RGSZ2 interaction reduces NO signaling. Impairment of RGSZ2 expression results in the overactivation of nNOS/NO-regulated NMDAR/calmodulin-dependent protein kinase II (CaMKII) cascade. This provokes a fast and lasting tolerance to morphine, comparable to the attenuation of opioid efficacy observed in states of persistent pain. Thus, RGSZ2 and NO emerge as potential targets to treatment of neural diseases in which abnormally strong NMDAR activity depresses that of the associated MOR.

of neural-specific PKCγ (36). This translocation raises the PKCγ activation threshold by reducing its sensitivity to local concentrations of diacylglycerol (DAG) (36), and it probably prevents the early potentiation of NMDAR, for example, before the strength of morphine signaling would require such control. Since the initial report associating PKC with MOR-dependent enhancement of NMDAR function (8), other elements have been seen to bridge the gap between these receptors. In this respect neural nitric oxide synthase (nNOS) exerts a well-established negative influence on MOR function (13, 22). This regulation is attributed to the NMDAR/nNOS cascade (20, 36), mainly because NMDAR activation or nitric oxide (NO) donors reduce the analgesic potency of morphine and accelerate the development of opioid tolerance (22). However, the nNOS that drives the MOR to NMDAR connection appears essentially to be recruited by MOR activity (39). Thus, the MOR-activated phosphoinositide 3-kinase (PI3K)/Akt cascade activates nNOS, carrying signals from the MOR toward the NMDAR. The PI3K/Akt/nNOS pathway acts upstream of PKC/Src and it plays a decisive role in the potentiation of NMDAR currents (39).

As observed for PKCγ in terms of the MOR to NMDAR connection (36), the morphine-induced potentiation of nNOS is counterbalanced by its translocation to the HINT1-RGSZ2 complex (39). Indeed, free zinc ions released by nNOS/NO facilitate the binding of PKCγ to HINT1, the cysteine-rich domain (CRD) in the PKCγ regulatory region physically associating with the histidine residues in the HINT1 protein. The association of nNOS with the MOR also requires the HINT1-RGSZ2 complex, although little is known about how this process occurs. Since nNOS lacks a CRD, the MOR-associated RGSZ2 protein rather than HINT1 could support this negative regulation. There is evidence indicating that RGSZ2 interacts with the MOR. The *RGSZ2* gene lies close to the *MOR* gene, suggesting that they may be coordinately expressed (25, 44), and, indeed, the *MOR* and *RGSZ2* genes are coregulated after voluntary oral morphine consumption and/or in the morphine-quinine two-bottle choice paradigm (11). Thus, RGSZ2 has been implicated in the development of morphine tolerance (35) and impaired RGSZ2 expression augments morphine analgesic activity, which is rapidly followed by sustained tolerance to its effects (15).

Significantly, nNOS is associated with the postsynaptic membrane through a PDZ domain at its N terminus (5), a region that is absent from the endothelial and inducible isoforms of the enzyme. This domain binds to the second PDZ domain of PSD-95 and couples nNOS to the NMDAR-mediated permeation of calcium fluxes that promote the formation of calcium-calmodulin (Ca^{2+}-CaM). Here we have examined how the PDZ domain affects the control of morphine-activated nNOS by RGSZ2 in PAG synaptosomes. We found that the nNOS PDZ domain binds to the PDZ-binding motifs upstream of the RGSZ2 RGS domain, and that this binding prevents Akt from enhancing the activity of the enzyme. In RGSZ2-deficient mice, the nNOS/NMDAR/calmodulin-dependent protein kinase II (CaMKII) pathway is excessively activated, and morphine antinociception is greatly reduced. These results reveal a critical role for the HINT1-RGSZ2 complex in the control of MOR-generated NO signaling.

Results

The N terminal PDZ domain of nNOS binds to the RGSZ2 PDZ domain binding motifs

Activation of PAG MOR is coupled to the Akt/nNOS/NO pathway (39), and after icv administration of 10 nmol morphine, increased cysteine S-nitrosylation of a series of MOR-associated proteins was detected *ex vivo*. However, no such modification was observed for the 60 kDa MOR itself (Fig. 1A).

Using antibodies characterized previously in mouse brain synaptosomes, we were able to detect the MOR, RGSZ2, and associated proteins. In PAG synaptosomes, the immunoprecipitated MOR was recognized by antibodies directed against different regions of the MOR sequence (Supplementary Fig. S1; Supplementary Data are available online at www.liebertonline.com/ars), and similarly, the RGSZ2 protein was also recognized by antipeptide antibodies whose epitopes lie in different regions on this protein (Supplementary Fig. S2). Morphine recruits nNOS to PAG synaptosomal membranes and to the MOR environment. While initially the nNOS-MOR association predominates after morphine administration, nNOS subsequently accumulates at the plasma membrane. The nNOS associated to the membrane but not to the MOR has been activated by the Akt-mediated phosphorylation of serine1417

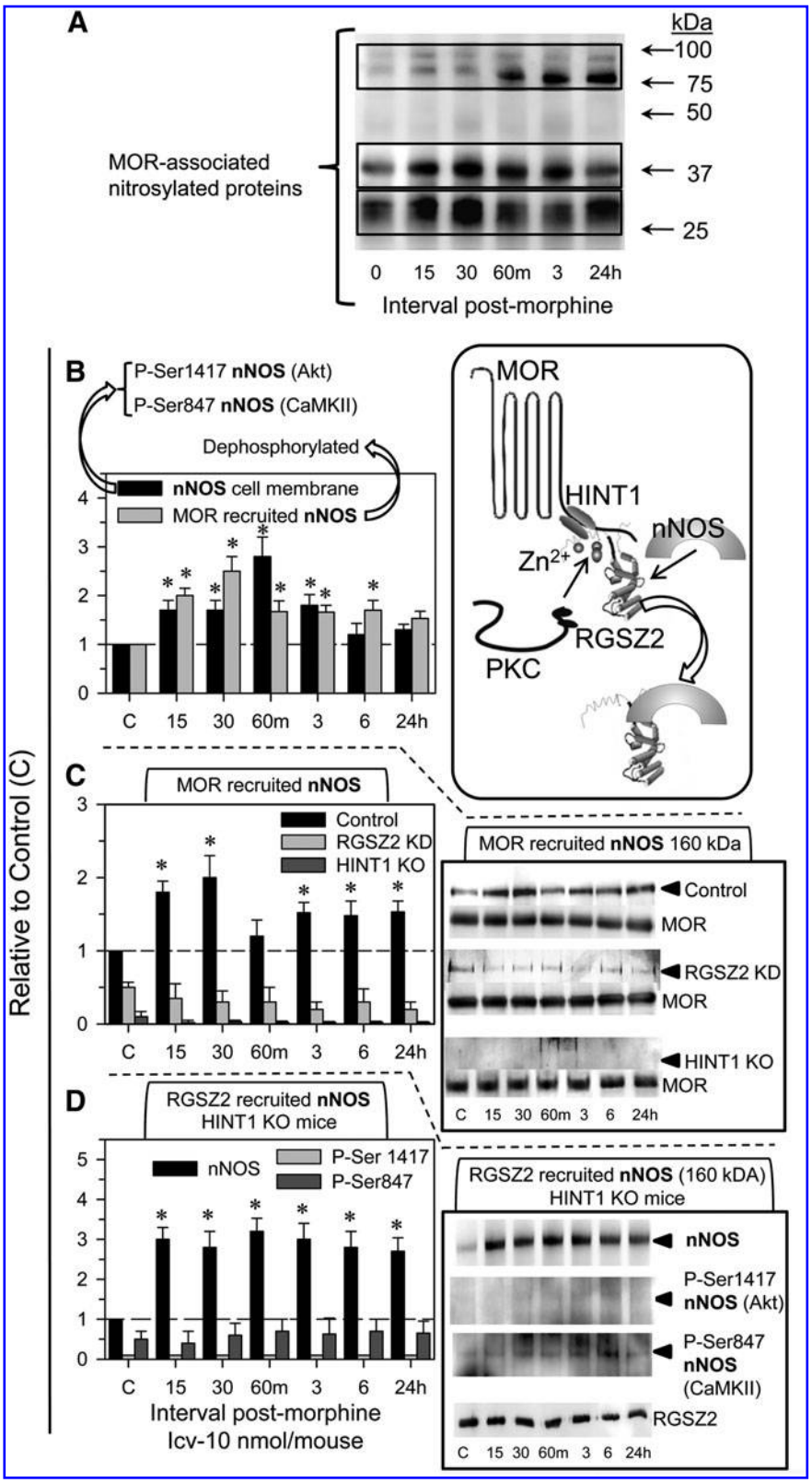

FIG. 1. Mu opioid receptor (MOR)-associated RGSZ2 control morphine-activated neural nitric oxide synthase (nNOS)/nitric oxide (NO) pathway. (A) The effect of morphine (10 nmol) administration *in vivo* on S-nitrosylation of MOR-associated proteins. At various intervals postinjection, groups of eight mice were sacrificed and their periaqueductal gray (PAG) were pooled for the *ex vivo* determinations. The MOR was immunoprecipitated (IP) and the presence of S-nitrosylated proteins was determined in Western blots. To assess antibody binding, the *areas* inside the *rectangles* of the same blot were subjected to different levels of exposition. **(B–D)** The effect of morphine (10 nmol) on nNOS at the synaptosomal PAG membrane and in the MOR environment. **(B)** After morphine administration, Akt-activating Ser1417 phosphorylation and calmodulin-dependent protein kinase II (CaMKII)-inactivating Ser847 phosphorylation were present in the membrane-associated pool of nNOS. The nNOS recruited to MOR environment lacked such phosphorylation (39) (see Supplementary Fig. S3). The membranes were resolved (40 μg protein/lane) by SDS-PAGE and the nNOS was determined at different postmorphine intervals in Western blots using the actin immunosignal as a loading control. The MOR was IP and the coprecipitated nNOS was evaluated using MOR signal as a loading control. Immunosignals were expressed as the change relative to the control animals that did not receive opioid (attributed an arbitrary value of 1, *dashed line*). Each data point is the mean of three assays performed on PAG samples obtained from independent groups of six mice each. The data are presented as the mean ± standard error of the mean (SEM). *Significantly different from the corresponding control group (C), $p < 0.05$. **(C)** Morphine-induced nNOS recruitment to the MOR: control mice, RGSZ2-deficient mice (KD: knockdown), and HINT1 (−/−) (KO: knockout) mice. *Inset*: representative Western blots. The data are the mean ± SEM from three determinations performed in PAG samples from different groups of six mice each. *Significantly different from the arbitrary value of 1 attributed to MOR recruited nNOS immunoreactivity control group (C); $p < 0.05$. **(D)** Morphine-induced binding of nNOS to RGSZ2 proteins in HINT1 KO mice. *Inset*: representative Western blots are shown. The nNOS recruited by morphine to the RGSZ2 protein lacked Akt-induced Ser1417 and CaMKII-mediated Ser847 phosphorylation. The data are the mean ± SEM from two determinations performed in PAG samples from different groups of three mice each. *Significantly different from the arbitrary value of 1 attributed to MOR recruited nNOS immunoreactivity control group (C at 0 time before morphine); $p < 0.05$. The signals corresponding to P-Ser1417/847 nNOS were almost no quantifiable. These data were referred to the value of nNOS control group C as well.

(Fig. 1B and Supplementary Fig. S3). Thus, during the early interval postmorphine administration the translocation of a fraction of nNOS to the MOR reduces the impact of Akt on this enzyme. At later intervals, CaMKII phosphorylates serine847 of nNOS, thereby reducing its activity (39). At the MOR CT, the RGSZ1 and RGSZ2 proteins associate with the HINT1 protein (2, 15). The absence of HINT1 or RGSZ2 proteins prevented nNOS from reaching the morphine-activated MOR (Fig. 1C). However, morphine still promoted the association of nonphosphorylated (serine 847, 1417) nNOS with RGSZ2 despite the lack of HINT1, although not at the MOR (Fig. 1D). Thus, targeted disruption of the *HINT1* segregates of RGSZ2 from the MOR, even though this RGSZ2 maintained its capacity to bind nNOS. These results suggested that RGSZ2 is the adapter protein that recruits nNOS to the MOR.

Immunohistochemical analysis revealed that RGSZ2 is widely expressed in PAG neurons, whereas those producing nNOS were much less abundant in this region. Importantly, the RGSZ2 protein colocalized with the nNOS enzyme, a generator of NO. Moreover, RGSZ2 immunoreactivity was distributed in dense spots along the plasma membrane, a pattern that is compatible with a regulatory role for RGSZ2 on GPCR function (Fig. 2). Eukaryotic Linear Motif (ELM: http://elm.eu.org/) analysis of RGSZ2 identified a series of PDZ binding motifs, 61–

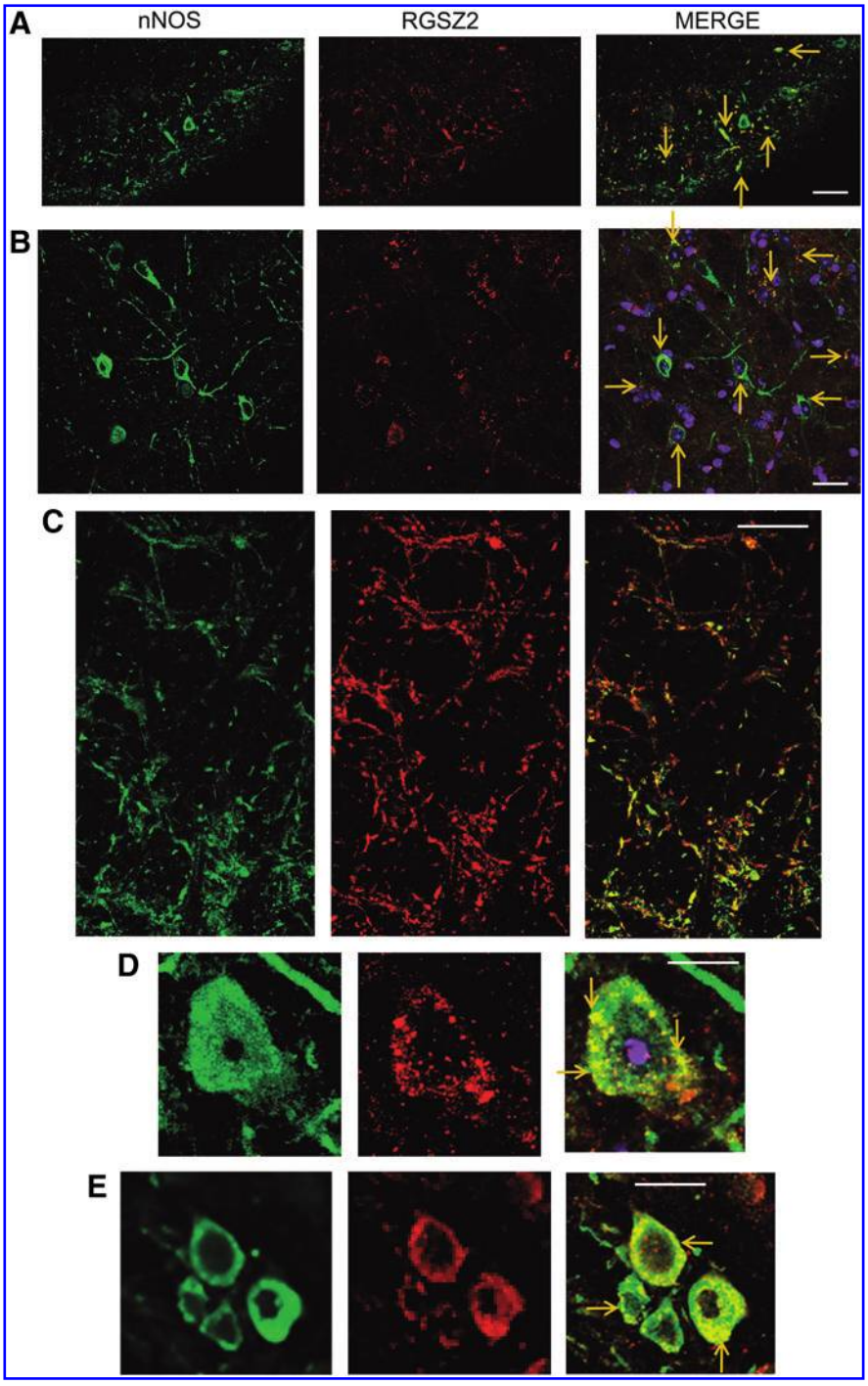

FIG. 2. Colocalization of nNOS and RGSZ2 in mouse PAG neurons. Confocal laser-scanning microphotographs taken from coronal histological sections through the midbrain PAG showing double immunostaining for nNOS (*green*) and for RGSZ2 antigens (*red*) in the ventrolateral column **(A–C)** and dorsal raphe nucleus **(D, E)**. The neuronal nNOS and RGSZ2 was observed with Alexa Fluor 488 and 568, respectively. Note that in the merged confocal microscopy images (*right panels*), several structures contain both the nNOS and RGSZ2 antigens. **(C)** Illustrates details of the colocalization between the nNOS and RGSZ2 antigens in the neuropil of the central PAG. **(D, E)** Represent high-power magnifications showing details of double-immunostained cells. Note the granular appearance of the RGSZ2 immunoreaction product in **(D)** and **(E)**. The *arrows* indicate structures that coexpress both nNOS and RGSZ2 antigens. Scale bars: **(A, B)** = 30 μm; **(C, D)** = 10 μm; **(E)** = 20 μm.

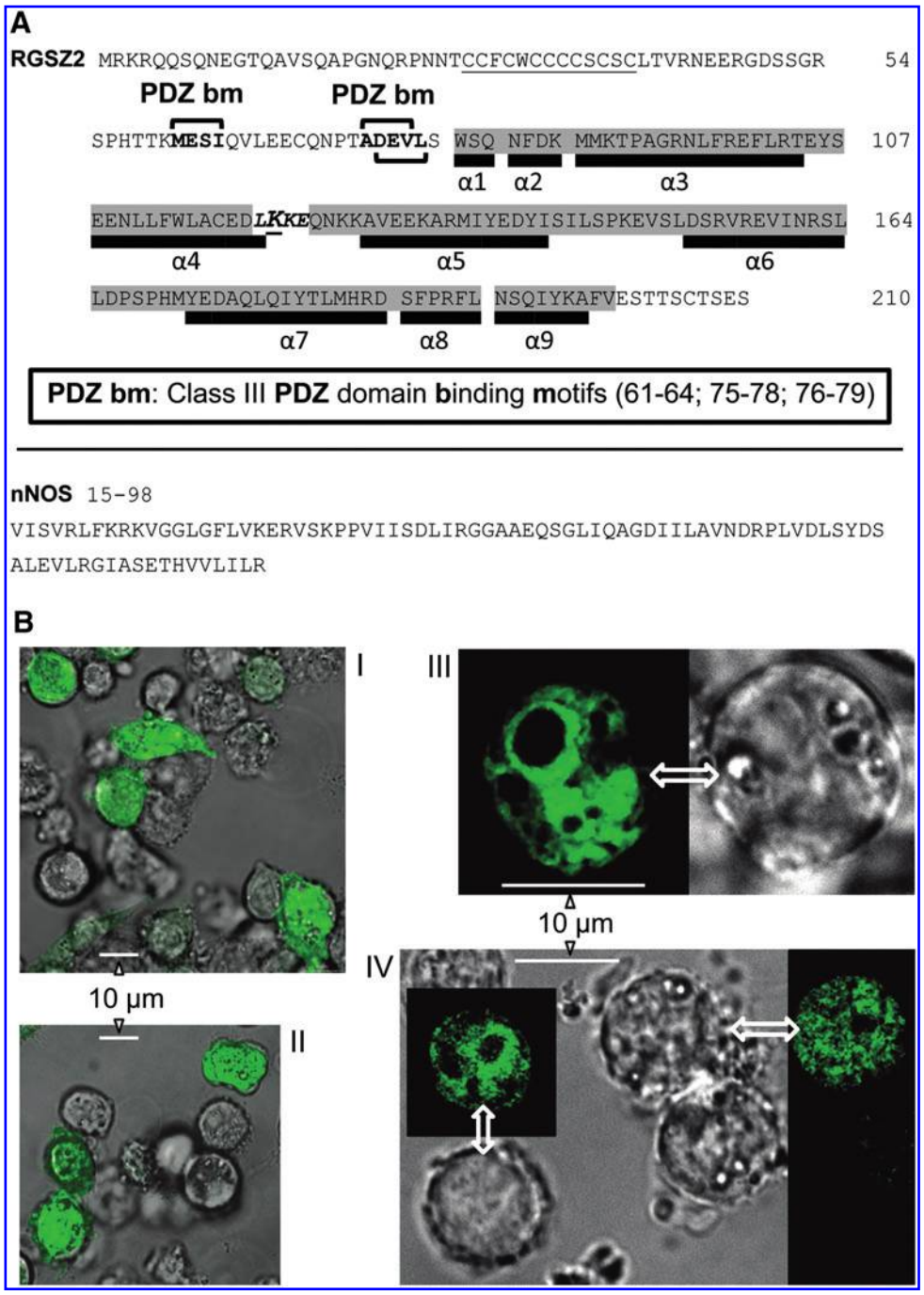

FIG. 3. Physical association of the RGSZ2 protein with the nNOS PDZ domain. (A) The RGSZ2 protein (AF191555.1) contains 210 residues with a cysteine-rich domain in its amino-terminus (residues 28–40) and the RGS domain (residues 80–190, comprised of nine alpha helices). ELM (http://elm.eu.org/) analysis of RGSZ2 revealed a series of PDZ domain binding motifs (bm); 61–64 MESI, 75–78 ADEV, and 76–79 DEVL. The amino acid sequence of the canonical nNOS (NP_032738.1) PDZ domain is shown. **(B)** Observation of RGSZ2 interaction with nNOS PDZ domain by BiFC. The CHO cells were transiently cotransfected with cDNAs encoding $RGSZ2^{VC155}$ and $nNOS^{VN173}$ (0.8 μg). The confocal signals are obtained after the direct physical association of both proteins provides that VC155 and VN173 assemble the active fluorescent molecule. **(I, II)** Phase field and fluorescent images are combined. **(III, IV)** The *arrows* indicate fluorescent image of positive cells in the field. Details as in Materials and Methods section.

64 MESI, 75–78 ADEV, and 76–79 DEVL, which could interact with the PDZ domain located at the nNOS N terminus (Fig. 3A). Thus, the *in vivo* formation of RGSZ2-nNOS complex was supported by the biomolecular fluorescence complementation (BiFC) analysis (Fig. 3B). The Chinese hamster ovary (CHO) cells were transfected with a mix (1:1) of RGSZ2 coupled to VC155 and of nNOS PDZ domain coupled to VN173 at the CT. In case these two proteins associate, the VC155 and VN173 fragments form a stable fluorescent complex, which was evident in several cells. Since these VC and VN fragments are not fluorescent on their own, the cells that in BiFC analysis did not fluoresce probably remained untransfected or they only expressed one of the proteins under study.

In *in vitro* pull-down assays and through Surface Plasmon Resonance analysis, we also observed a direct physical interaction between recombinant murine RGSZ2 and the canonical nNOS 15–98 PDZ domain. This interaction was lost in mutated RGSZ2 E62A + S63G or RGSZ2 D76A + E77A + V78G (Fig. 4A–C). *In vitro*, wild-type (WT) RGSZ2 had a biphasic effect on nNOS activity. At concentrations below those of nNOS (50 n*M*), RGSZ2 moderately increased its enzymatic activity, whereas when the RGSZ2 concentration was greater or equal to that of nNOS its activity was greatly reduced (Fig. 4D). Thus, the N terminal PDZ domain of nNOS binds to internal peptide sequences of RGSZ2 (PDZ binding motifs), an interaction that mostly impairs nNOS activity.

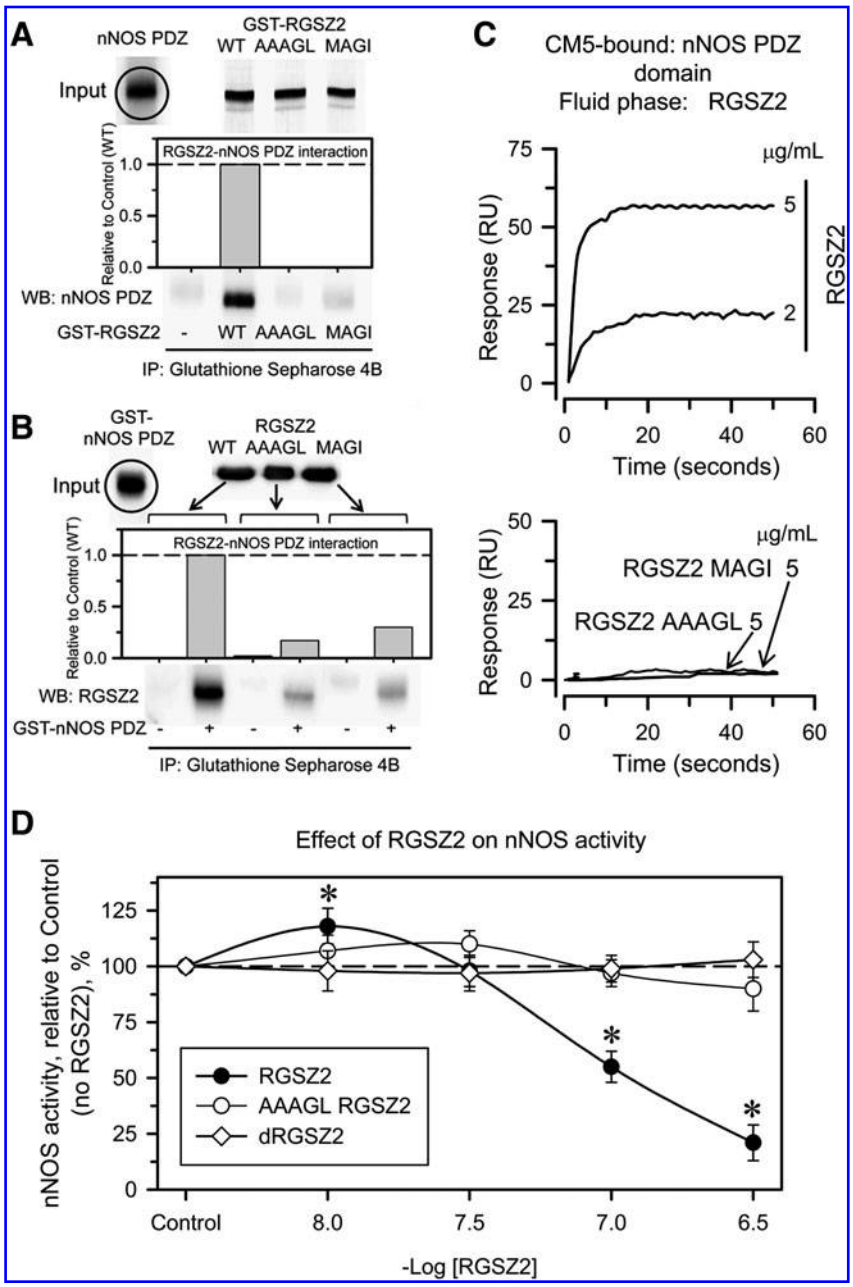

FIG. 4. Interaction between recombinant wild-type and mutated RGSZ2 protein with the nNOS PDZ domain. *In vitro* nNOS PDZ binds to wt RGSZ2 but not to its mutants. Coprecipitation assays: recombinant RGSZ2 (200 n*M*) was incubated with 200 n*M* of nNOS (aa: 15–98). **(A)** GST-RGSZ2 variants were precipitated with Glutathione-Sepharose and the associated nNOS was evaluated. **(B)** GST-nNOS (15–98) was pulled down and the associated RGSZ2 evaluated. **(C)** Surface plasmon resonance analysis: the nNOS N terminal PDZ domain was covalently anchored to CM5 chip and wild-type RGSZ2 protein bound to the nNOS PDZ. Mutated 61–64 MAGI and 75–79 AAAGL RGSZ2 displayed no affinity toward the nNOS PDZ. **(D)** WT RGSZ2 decreases the activity of the full nNOS sequence *in vitro*. The nNOS (50 n*M*) was incubated with RGSZ2 variants (10–300 n*M*) and the mutated AAAGL RGSZ2 and the RGS domain alone did not affect this enzymatic activity. Each data point is the mean ± SEM from two independent assays performed in duplicate. *Significantly different from the Control nNOS group; $p < 0.05$.

RGSZ2 prevents morphine from producing rapid and long-lasting analgesic tolerance

Neural RGSZ2 is a sumoylated and glycosylated protein, and while RGSZ2 knockout (KO) mice are available, previously characterized synthetic end-capped phosphorothioate antisense oligodeoxynucleotides (ODNs) were used to silence the expression of the RGSZ2 protein (15). This procedure reduces the MOR-associated RGSZ2 by about 50%–70% (Supplementary Fig. S4), without affecting the expression of RGSZ1, G proteins or MOR (15). A single icv dose of about 10 nmol morphine per mouse is suitable to promote MOR desensitization, whereas smaller doses (*e.g.*, 3 nmol morphine) only produce moderate single-dose tolerance [see *e.g.*, Garzón *et al*. (15)]. As reported previously in RGSZ2-deficient mice, 10 nmol morphine elicits a stronger analgesic effect during the early postopioid interval, followed by a rapid desensitization during the time-course of morphine analgesia (see Fig. 5A). However, the analgesia evoked by a second and identical dose of morphine 24 h later was clearly diminished in both RGSZ2-deficient and WT mice. Indeed, in RGSZ2-knockdown mice, the second dose of morphine lacked the initial sharp response and the peak effect was now observed closer to the 30 min postopioid interval. Control mice desensitized by administration of 10 nmol morphine recovered the morphine analgesic response 48 h later, reaching baseline levels after 4–5 days. However, in the absence of RGSZ2 the analgesic response remained dampened over this period (Fig. 5B). In a parallel group of mice that received ODN injections on 5 days there was a gradual recovery of the protein when

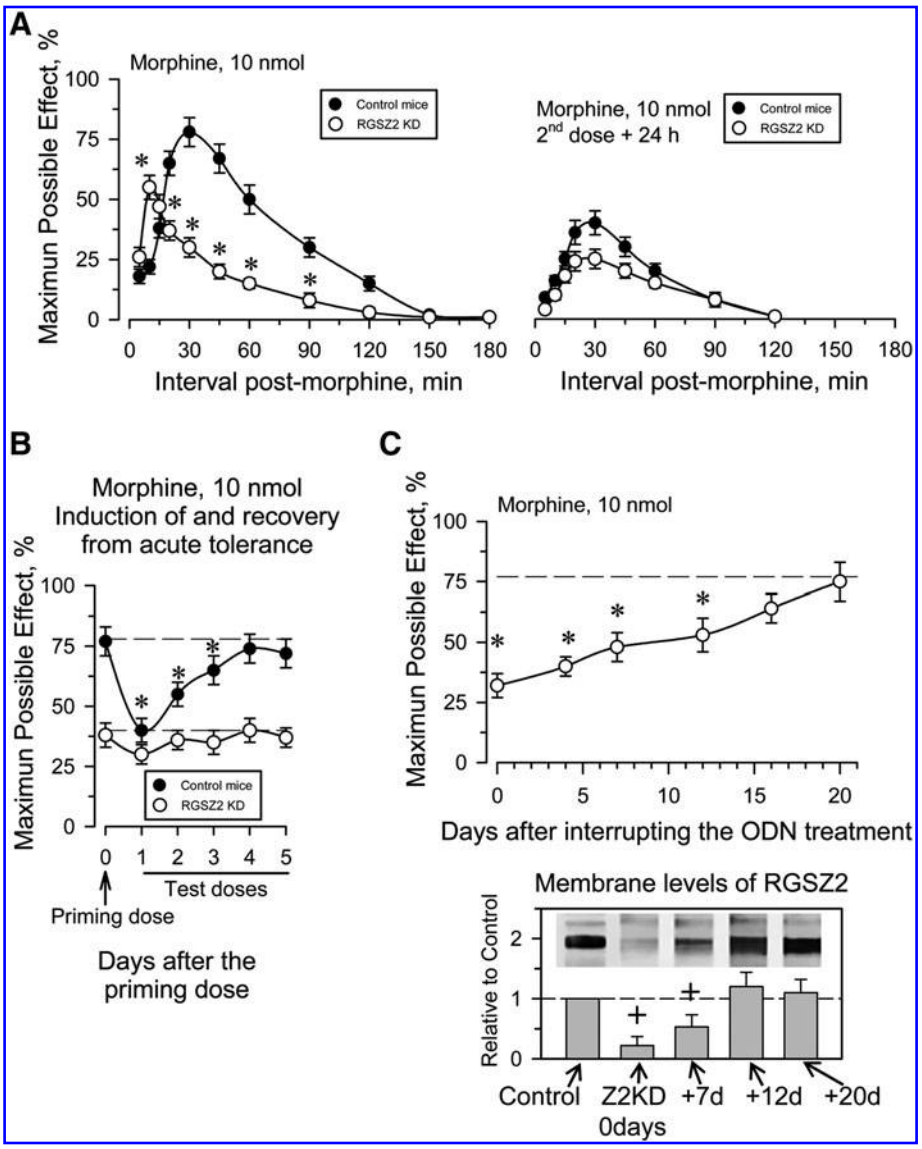

FIG. 5. Influence of RGSZ2 KD on morphine's analgesic activity. **(A)** RGSZ2-deficient mice were prepared by oligodeoxynucleotide (ODN) administration over 5 days (15), on day 6 they received intracerebroventricularly (icv) 10 nmol morphine, and a second identical morphine dose 24 h later. Antinociception was determined by the warm water (52°C) tail-flick test at various time intervals post-injection. The values are the mean ± SEM from groups of eight mice. *Significantly different from the control group that received the mismatched ODN, $p < 0.05$. KD: RGSZ2 KD mice. **(B)** Time-course of acute analgesic tolerance produced by a single dose of morphine. During the days that followed the initial 5 day ODN administration (15), RGSZ2 levels were maintained low by a daily injection of 3 nmol ODN. The tail-flick test was conducted 30 min after injection of the 10 nmol priming morphine dose on day 6 (indicated as 0 in the graph). After the priming dose, every 24 h a different group of mice received a test dose of 10 nmol morphine and analgesia was subsequently evaluated 30 min later. *Significantly different from the control group that only received the priming dose of the agonist (0 days, *dashed lines*, $p < 0.05$). **(C)** Recovery of RGSZ2 and the analgesic response to morphine. After the initial 5 days of ODN administration (15) the RGSZ2-KD mice received no additional ODN doses and the levels of this protein were monitored for several days. The effect of RGSZ2 recovery on analgesia was analyzed. After the priming morphine dose on day 6 (indicated as 0 in the graph), a different group of these mice received a test dose at the intervals indicated in the figure and analgesia was evaluated 30 min later. *Significantly different from the control group that only received the priming dose of the agonist (*dashed line*, $p < 0.05$). Membrane levels of RGSZ2 were determined before the ODN treatment (control), at the end of the 5-day ODN treatment (Z2KD 0 days) and 7, 12, and 20 days after treatment. Each bar is the mean of three assays performed on PAG samples obtained from independent groups of six mice each. Data are means ± SEM. †Significantly different from the control group that received the active ODN treatment against RGSZ2 mRNA ($p < 0.05$).

the treatment was suspended, as well as recovery of the analgesic response to morphine that was complete after ~2 weeks (Fig. 5C).

RGSZ2 reduces the impact of morphine-activated nNOS/NO on NMDAR-CaMKII pathway

Before icv morphine injections of RGSZ2-deficient mice, the membrane levels of nNOS and of its activating Akt-mediated Ser1417 phosphorylation were almost identical to that of control mice. By contrast, CaMKII-mediated Ser847 phosphorylation was clearly weaker. In RGSZ2-deficient mice morphine increased the membrane levels of nNOS and of its activating Ser1417 phosphorylation for longer than in control mice, in conjunction with reduced nNOS inactivating Ser847 phosphorylation (Fig. 6). Thus, silencing the MOR-associated RGSZ2 protein weakened the MOR's negative influence on nNOS activity.

Morphine did not increase the presence of the MOR in the cytosolic fraction of PAG synaptosomes in either control or RGSZ2-deficient mice (Fig. 7A). The experimental reduction of RGSZ2 levels brought about the hyper-phosphorylation of the MOR. Nonetheless, the serine 375 that has been linked to GRK2- and arrestin-mediated internalization of the MOR was not phosphorylated (42). Notably, the NMDAR-CaMKII pathway was strongly activated, as evident through the

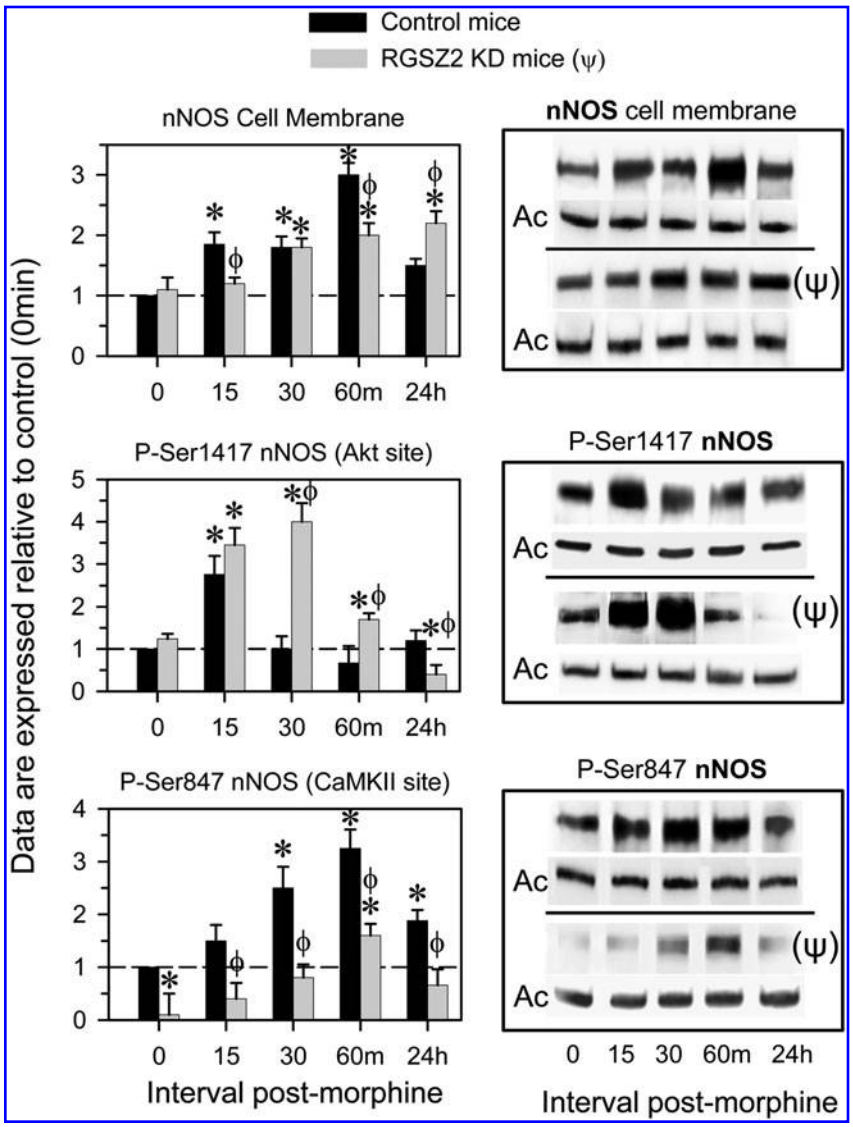

FIG. 6. De-regulation of morphine-activated nNOS in RGSZ2-deficient mice. Experimental silencing of RGSZ2 influences the regulation of nNOS activity at the cell membrane by morphine. Morphine (10 nmol) was icv-injected on day 6 to control (mismatched ODN) and RGSZ2-KD mice (ψ, after 5 days of ODN treatment). Before and at various intervals postinjection, groups of eight mice were sacrificed, and the PAG were collected for the *ex vivo* determination of nNOS in PAG synaptosomal membranes. The data corresponding to control mice at 0 min (before morphine icv injection) were assigned an arbitrary value of 1 (*dashed lines*), and those of the post-morphine intervals were expressed relative to this value. The data obtained in RGSZ2 KD mice (before and after morphine) were also referred to those controls. The bars are the mean ± SEM of three independent determinations performed in different groups of mice. *Significantly different from the control group (0 min) that had received the mismatched RGSZ2 ODN; $^{\varphi}$Significantly different from the control group at the indicated post morphine interval, $p < 0.05$. Representative blots are shown. Equal loading was verified by assaying actin (Ac). Further details in Figure 1.

phosphorylation of the NMDAR subunits and of CaMKII (Fig. 7B, C).

In the absence of RGSZ2, disruption of the nNOS/PKC/NMDAR/CaMKII pathway restores the function of the MOR and rescues morphine analgesia

Those changes brought about by RGSZ2 knockdown in the PAG MOR-NMDAR connection were dampened by *in vivo* inhibition of nNOS, PKC, CaMKII, or by antagonism of the glutamate-driven NMDA receptor. Therefore, MOR serine phosphorylation, CaMKII Thr286 autophosphorylation, as well as the phosphorylation of Tyr416 nonreceptor tyrosine kinase (Src/Fyn) and Tyr1325 NMDAR2A all diminished within few minutes of treating the mice with the corresponding compounds (Fig. 8A, B). In control mice, the icv injection of nNOS inhibitors (7 nmol L-NNA; 20 nmol L-NAME), PKC inhibitors (1 nmol Gö7874; 15 n*M* Chelerythrine), CaMKII inhibitor (10 nmol KN93), or NMDAR antagonists (1 nmol MK801; 3 nmol D-AP5) a few minutes before the initial dose of 10 nmol morphine produces only small changes in the analgesia observed (40). However, these treatments did restore the analgesic potency of morphine in RGSZ2-deficient mice (Fig. 8C).

Discussion

The nNOS/NO pathway supports the cross-regulation between the MOR and NMDAR in the control of nociception (32). Morphine regulates the enzymatic activity of nNOS by a push–pull mechanism, whereby it promotes nNOS activation *via* the MOR/PI3K/Akt pathway and it diminishes NO production by protecting nNOS from the effects of Akt (39). Our results indicate that morphine-induced production of NO is efficiently counterbalanced by nNOS binding to the MOR-coupled RGSZ2 protein. The MOR bears the HINT1-RGSZ2 complex in its CT, and while HINT1 elimination abolishes nNOS recruitment to the MOR, it increases morphine effects but it does not prevent morphine from producing analgesic tolerance (18, 36). Therefore, morphine induces nNOS binding to RGSZ2 proteins, and in absence of HINT1 this complex is formed but separated from the MOR. The nNOS-RGSZ2 interaction controls NO signaling and accordingly, disruption of this association results in the overactivation of nNOS/NO-regulated signaling pathways

(*e.g.*, the NMDAR/CaMKII cascade), provoking fast and lasting tolerance to morphine. In these circumstances, strong serine phosphorylation of the MOR probably prevents it from productively regulating of G proteins, thereby contributing to the long-lasting, weak analgesic effects of morphine.

The specificity of NO signaling is regulated by the targeting of nNOS to the precise neuronal environment. This is achieved by means of adapter proteins that interact with its PDZ domain. The cytoskeletal protein PSD95/93 links nNOS to the NR2 subunits of NMDAR, whereas the carboxy-terminal PDZ ligand of nNOS (CAPON) links nNOS to synapsin and Dexras1. Other proteins like PIN, NOSIP, Hsp90, and caveolin-3 bind outside the PDZ domain and they apparently either regulate NO production or modulate the localization of nNOS (49). The canonical nNOS PDZ domain contains ~100 amino-acid residues, forming a compact globular structure of a six-stranded antiparallel β-barrel flanked by two α-helices able to bind either the carboxyl-terminal sequences of proteins or internal peptide sequences. The interaction between a PDZ domain and its target may be constitutive; however, agonist-dependent activation of cell surface receptors is sometimes required to promote interaction with PDZ proteins. The nNOS PDZ-containing N terminus facilitates the regulatory binding of this enzyme to the MOR-coupled RGSZ2 protein. This canonical nNOS PDZ domain binds to an internal peptide sequence in RGSZ2 upstream of the RGS domain that fulfils the D-X-V requirement (45). This type of PDZ interaction is promoted by GPCR activation, and thus, after acting on the MOR, morphine promotes the activation of the PI3K/AKT/nNOS pathway and the binding of nNOS to RGSZ2 at the MOR CT. Since active nNOS forms a homodimer (10), the binding of RGSZ2 could alter the productive formation of the nNOS complex.

In PAG neurons, morphine-activated MOR increases NMDAR-induced calcium fluxes by the concatenated activation of PI3K/Akt/nNOS pathway (39). NO promote the release of zinc ions from endogenous stores, for example, metallothioneins, which is required for the binding of inactive PKCγ to the HINT1-RGSZ module at the MOR CT (36). This action reduces PKCγ sensitivity to local concentrations of DAG, enabling it to be regulated by morphine-released G$\beta\gamma$ dimers that act on PLCβ to produce the DAG and calcium ions needed to activate this kinase (30). Subsequently, PKCγ recruits Src to phosphorylate NMDAR subunits (6, 7, 38), contributing to the sustained potentiation of NMDAR-mediated glutamate responses (8, 24, 31). This provokes the activation of CaMKII, which directly or indirectly uncouples MOR from its regulated

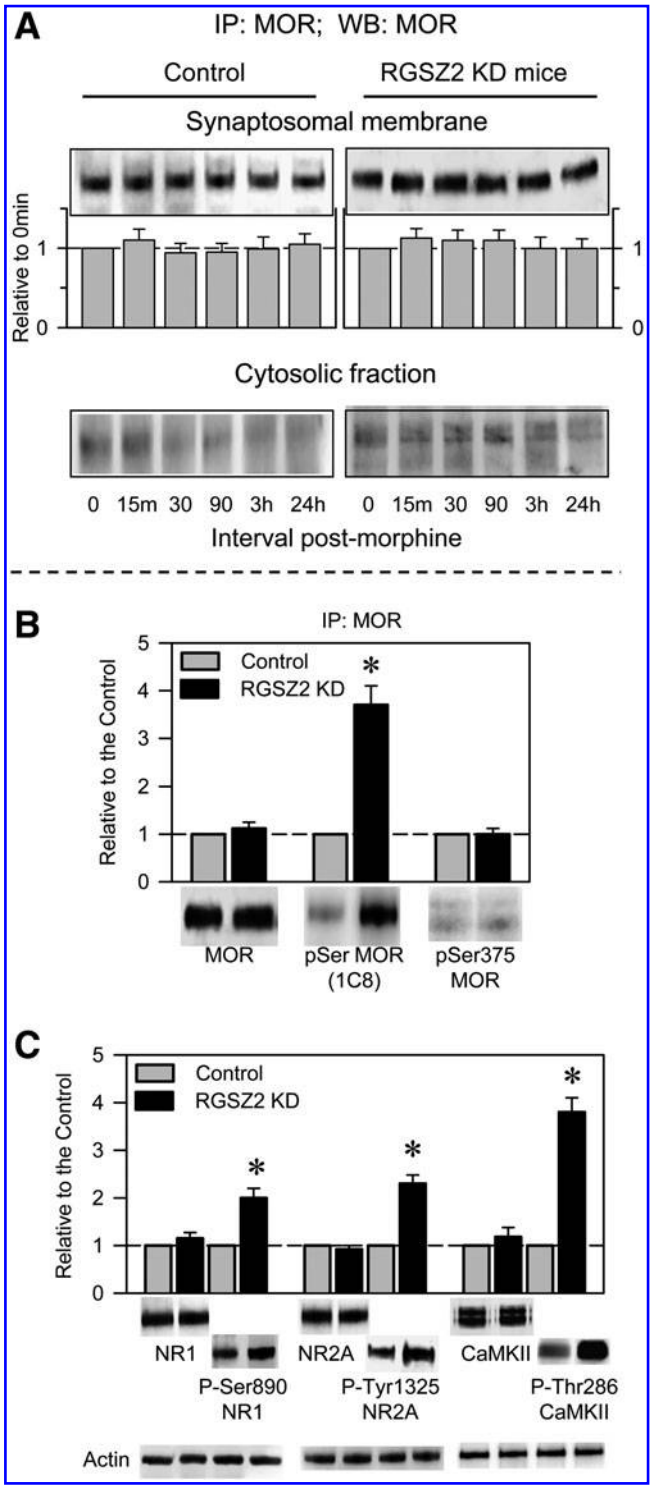

FIG. 7. RGSZ2 Impairment induces changes in MOR-regulated proteins: effect of morphine. (A) icv morphine (10 nmol) does not induce a significant change in the MOR present in PAG synaptosomal membrane preparation of either control or RGSZ2-KD mice. No significant increase of the MOR population could be appreciated in the corresponding cytosolic fraction. The MOR was IP from PAG synaptosomes at the postopioid intervals indicated and subsequently quantified in Western blots. The faint signals of the cytosolic MOR could not be accurately quantified. **(B, C)** The effect of RGSZ2 impairment on MOR and MOR-regulated proteins was studied in absence of morphine. **(B)** The MOR was IP from PAG synaptosomes and serine phosphorylation of surface MORs was determined under denaturing conditions (clone 1C8 and p-Ser375 MOR). Since morphine promotes no internalization of the MOR these signals were used to control for loading. The control was assigned an arbitrary value of 1 and the data are presented as the mean ± SEM of three assays performed on PAG samples obtained from independent groups of four mice each. *Significantly different from the control group that had received the mismatched RGSZ2 ODN, *dashed line*, $p < 0.05$. Representative blots are shown. **(C)** Phosphorylation of NMDAR1/2A subunits and of CaMKII was evaluated in PAG synaptosomes. Equal loading was verified by assaying actin. Details as in **(B)**.

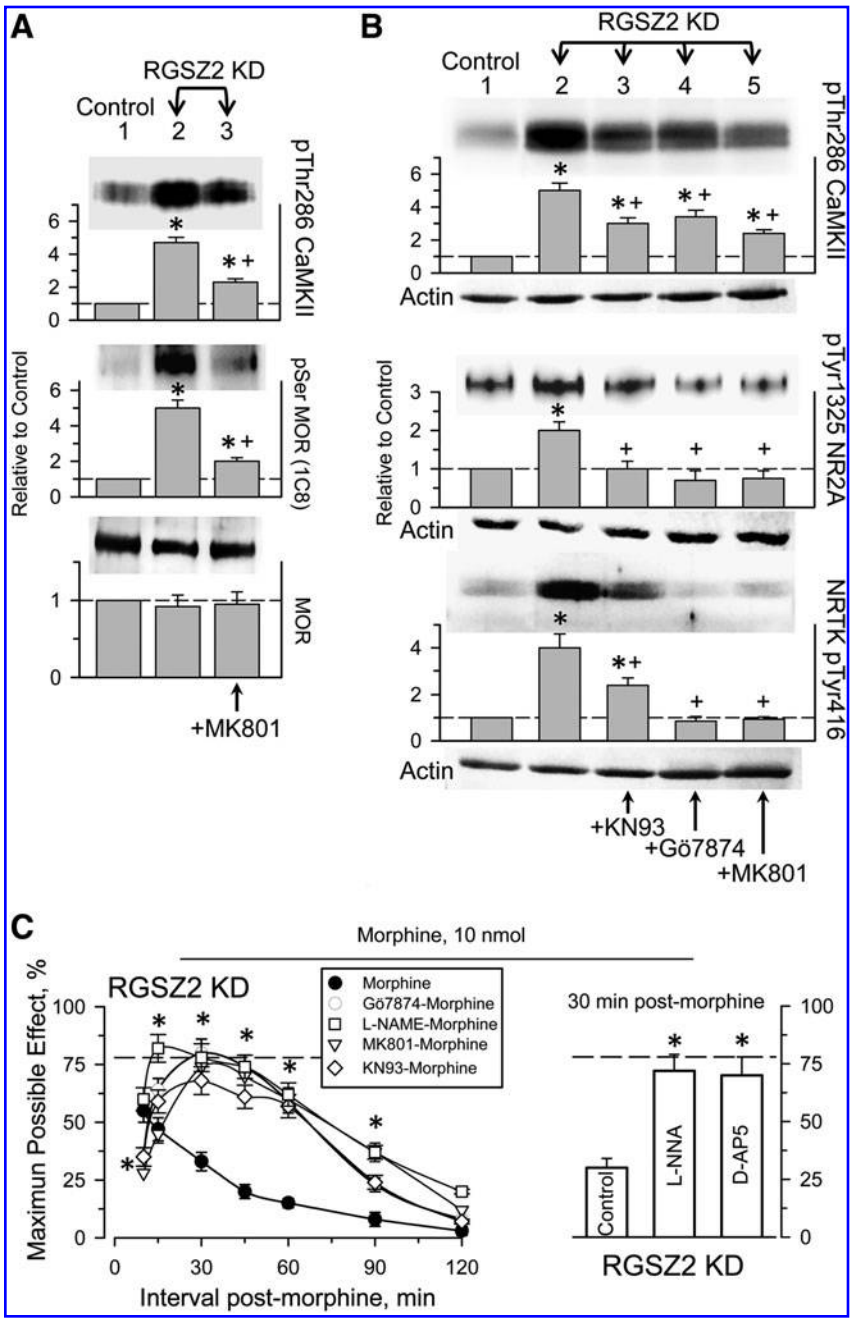

FIG. 8. Disruption of MOR-NMDAR cross-regulation restored morphine analgesia in RGSZ2-KD mice. (A, B) The PKC inhibitor (1 nmol Gö7874), NMDAR antagonist (1 nmol MK801) or CaMKII inhibitor (10 nmol KN93) were icv-injected in mice with reduced levels (KD) of RGSZ2 protein. The animals were sacrificed 30 min later to obtain PAG synaptosomes. **(A)** Effect of MK801 on pThr286 CaMKII and MOR serine phosphorylation. **(B)** The effect of KN93, Gö7874, and MK801 on pThr286 CaMKII, pTyr1325 NMDAR2A, and pTyr416 nonreceptor tyrosine kinases was determined in PAG synaptosomal membranes. **(A, B)** The values are the mean ± SEM of two-three assays performed on PAG samples obtained from groups of four mice each. *Significantly different from the control group that received the mismatched RGSZ2 ODN, assigned an arbitrary value of 1, *dashed lines*; †significantly different from the RGSZ2 KD group not receiving the pharmacological treatment (lane 2), $p < 0.05$. **(C)** Inhibition of nNOS/PKC/NMDAR/CaMKII on morphine-induced antinociception in RGSZ2-deficient mice. Groups of mice were icv-injected with the inhibitors or vehicle 30 min before treatment with 10 nmol morphine. Antinociception was determined by the warm water (52°C) tail-flick test and the values represent the mean ± SEM of groups of 12 mice each. The effects of Gö7874 (PKC inhibitor), L-NAME (nNOS inhibitor), MK801 (NMDAR antagonist), and KN93 (CaMKII inhibitor) were evaluated on the time-course of morphine analgesia. The activity of L-NNA (nNOS inhibitor) and that of D-AP5 (NMDAR antagonist) were studied 30 min postopioid administration. Each bar point is the mean ± SEM, $n = 8$ mice. The *dashed line* indicates the morphine analgesic peak effect observed for the control group no reveicing the ODN treatment. *Significantly different from the RGSZ2-KD group that received morphine and the vehicle instead of the kinase inhibitor, $p < 0.05$.

transduction and favors the development of morphine tolerance (40). This regulatory loop is blocked by nNOS inhibition (39), PKC inhibition, NMDAR antagonism, and CaMKII inhibition [reviewed in Garzón *et al.* (16)]. These pharmacological interventions restore the coupling of MOR to G proteins, but they uncouple MOR from the nNOS/PKC/NMDAR pathway, whereby morphine maintains its analgesic potency.

In the absence of morphine, the phosphorylation of signaling proteins implicated in the MOR-NMDAR connection increases in PAG synaptosomes from RGSZ2-deficient mice. This is probably a consequence of endogenous substances, opioids included, acting on GPCRs functionally coupled to NMDARs *via* PKC/Src (16, 26). Such abnormal increases in protein phosphorylation were efficiently reduced by restoring RGSZ2 levels and through pharmacological approaches, such as the inhibition of nNOS, PKC, NMDAR, or CaMKII. These treatments disrupt the hyperactivity of the NMDAR/CaMKII pathway and restored the potency of morphine. Therefore, RGSZ2 dysfunction affects nNOS/NO, PKC, NMDAR, and CaMKII, which act in the negative feedback loop that controls morphine-activated MOR signaling.

In the light of these data, NO is clearly implicated in the hyperactivation of the NMDAR/CaMKII cascade in RGSZ2-deficient mice. The loss of RGSZ2 unleashes nNOS activity, increasing NO levels and probably the presence of free zinc ions. Moreover, disruption of the HINT1-RGSZ2 complex prevents zinc-mediated recruitment of inactive PKCγ to the MOR environment (36). When liberated of the negative influence of the MOR, PKCγ is more rapidly activated, and since

high zinc stabilizes the binding of DAG to PKC regulatory domain, this activation persists for longer (36). These changes contribute to the abnormal enhancement of NMDAR/CaMKII function mediated by PKC/Src. On the other hand, nNOS also contributes to overregulation of NMDAR signaling in those RGSZ2-deficient mice by participating in MOR-extracellular signal-regulated kinase (ERK)1/2 pathway (1, 4). Indeed, NO can directly activate H-Ras (19), and the nNOS-CAPON complex activates Dexras1 (49). As a result, the Ras/Raf-1/MEK/ERK1/2 cassette becomes active (48). ERK1/2 activity increases the surface expression of GluR1 and GluR2L subunits of the glutamate-driven α-amino-3-hydroxy-5-methyl-4-isoxazole propionic acid receptor, which contributes to the enhancement of NMDAR activity and to long-term potentiation of the postsynapse (33, 50). Consequently, the increased activity of nNOS in absence of RGSZ2 promotes NMDAR-mediated fast MOR desensitization and long-term analgesic tolerance to morphine develops.

The MOR-NMDAR relationship explains the clinical efficacy of NMDAR antagonists in reducing opioid tolerance and their successful use in diminishing the consumption of analgesics (21, 27). Pharmacological, electrophysiological, and behavioral studies have demonstrated a relevant role of the NMDAR in the genesis and/or maintenance of chronic/persistent pain states (3, 14). The attenuation of opioid efficacy observed in states of persistent pain appears to be caused by abnormally strong NMDAR activity. Therefore, the genesis and/or maintenance of persistent pain could arise from alterations to MOR/NO/PKC/NMDAR coupling. Silencing of the MOR-associated RGSZ2 helps increase nNOS/NMDAR activity and it promotes profound and lasting morphine-induced MOR desensitization. Thus, RGSZ2 emerges as a potential target to treatment of neural diseases in which an enhanced NMDAR activity depresses that of the associated GPCR.

Materials and Methods

Preparation of recombinant proteins

Constructs of the murine full-length RGSZ2 (AF191555) and the PDZ domain of murine nNOS (NM_008712.2) were generated by polymerase chain reaction (PCR) using mouse PAG cDNA as a template (High Fidelity PCR enzyme mix; Fermentas # K0191). The primers included *Sgf*I and *Pme*I restriction sites and corresponded to the 5′ and 3′ ends of the coding region: RGSZ2-specific primers: 5′-GACCGC GATCGCCAGAAAACGGCAGCAGTCACA-3′ (forward) and 5′-GATGGTTTAAACTTAGGATTCAGAAGTACAGCT GGTG-3′ (reverse); nNOS primers: 5′-AGGAGCGATCGC CATGCAGATCCAACCCAACGTCATT-3′ (forward) and 5′-GATGGTTTAAACTTAAACATCCCCTGTGAAGGTG-3′ (reverse). Glutathione S-transferase (GST) fusion proteins were generated by inserting the PCR product into the pFN2A (GST) Flexi vector (Promega, #C8461) at the *Sgf*I and *Pme*I sites. The vector was introduced into *Escherichia coli* BL21 (KRX; Promega, #L3002) and the GST fusion proteins were purified on glutathione-sepharose 4B columns (GE Healthcare Bio-Sciences, #27-4570). The proteins retained were eluted with a 0–20 m*M* glutathione gradient as GST fusion proteins, or they were cleaved in the column with ProTEV protease (Promega, #V605A).

Site-directed mutagenesis of the RGSZ2 protein (Glu 62 to Ala and Ser 63 to Gly) was performed by PCR mutagenesis using the following primers: 5′-CCAAAATGG***C***G***G***GCATC CAGGTCCTAGAGGAATGCC-3′ (forward) and 5′- CTGG ATGC***G******C***CCATTTTGGTGGTATGTGGGG-3′ (reverse) (point mutations indicated in bold/italic). Mutation of Asp 76 to Ala, Glu 77 to Ala, and Val 78 to Gly was achieved with the primers: 5′-CTGCAG***C***TG***C***AG***G***CTTGTCCTGG-3′ (forward) and 5′-GGACAAG***G***CT***C***CA***C***CTGCAGTGGGGTTTTGG-3′ (reverse). The amplified fragments were digested with *Sgf*I and *Pme*I and cloned into the pFN2A (GST) Flexi vector (Promega, #C8461). The plasmid sequences and point mutations were confirmed by automated capillary sequencing.

BiFC analysis

The plasmid pPD49.83 was used to generate two cloning vectors for BiFC analysis. Constructs containing *hsp-16.41* heat shock promoter, an Myc or hemagglutinin tag for detection of BiFC fusion proteins, a multiple cloning site, a linker sequence, and the N-terminal fragment of Venus truncated at residue 173 (VN173) or the C-terminal fragment of Venus starting at residue 155 (VC155), were generously provided by Dr. Chang-Deng Hu (Purdue University). Full-length murine RGSZ2 and the PDZ domain of nNOS were subcloned in-frame into pCE-BiFC-VC155 or pCE-BiFC-VN173 plasmids using standard cloning strategies. Fragments were PCR amplified using the following primers: RGSZ2, AGC*G/TCGAC*GAGAAAACGGCAGC and *GGTAC/C*TGAAAATTAGGATTTAGAA for pCE-BiFC-VC155, and PDZ nNOS, TCTG*G/AATTC*TTCTGTCC GTCTCTTCAAACGC and ACTT*G/TCGAC*CAGGGCCTCT CAGAATGA for pCE-BiFC-VN173 plasmid. CHO cells were grown in Dulbecco's modified Eagle's medium, supplemented with 1 m*M* sodium pyruvate, 2 m*M* L-glutamine, 100 U/ml streptomycin, 100 μg/ml penicillin, and 10% (v/v) fetal bovine serum at 37°C in an atmosphere of 5% CO_2. Cells were transfected at ~70% confluence using Lipofectamine 2000 (Invitrogen) according to the manufacturers' protocol. The cells were further incubated for 18–36 h before testing for transgenic expression. Samples were observed on glass-bottomed plates (MatTek Co) on a Leica DMIII 6000 CS confocal fluorescence microscope equipped with a TCS SP5 scanning laser.

RGSZ2-nNOS interaction

RGSZ2 (200 n*M*) and nNOS (15–98) (200 n*M*) were incubated alone (negative control) or together in 450 μL of buffer (10 m*M* HEPES, pH 7.4, 150 m*M* NaCl, 3 m*M* EDTA, and 0.005% P20) mixed by rotation for 30 min at room temperature. Glutathione sepharose 4B (GE Healthcare Bio-Sciences AB #17-0756-01) beads were added, and after mild centrifugation, the pellets were washed three times and solubilized in 2× Laemmli buffer. The presence of RGSZ2 or nNOS (15–98) was analyzed by Western blots.

Surface plasmon resonance analysis of RGSZ2 and nNOS interactions was carried out on a BIACORE X (GE Healthcare Bio-Sciences). The PDZ domain of nNOS (50 μg/ml) was amine-coupled to channel 2 of a CM5 sensor chip (GE, BR-1000-14) and channel 1 was the blank. The sensor surface was equilibrated with HBS-EP buffer (GE, BR-1001-88) and sensorgrams were collected at 25°C at a flow rate of 10 μL/min following the passage of RGSZ2 (75 μL). The CM5 sensor chip was regenerated after each cycle with two 15 μL pulses of 10 m*M* glycine provided at 30 s intervals (pH 2.5, GE, BR-1003-56). Increasing analyte concentrations were studied

and the results were plotted using BIAevaluation software (v 4.1).

Effect of RGSZ2 on nNOS activity

The activity of recombinant nNOS (Alexis Biochem., ALX-201-028) was monitored by the conversion of arginine to citrulline. The nNOS (50 n*M*) was incubated for 10 min at 25°C with increasing concentrations of RGSZ2 (10–300 n*M*), and the NOS was assayed (Calbiochem, 482700) with ^{14}C-arginine (Amersham CFB63, 319 mCi/mmol) in a final volume of 50 μL containing: 50 m*M* Tris-HCl pH 7.4, 3 μM tetrahydrobiopterin, 1 μM FAD and 1 μM FMN, 1 m*M* NADPH, 0.6 m*M* $CaCl_2$, ^{14}C-arginine (50 μCi/ml), and 0.1 μM calmodulin. The NOS inhibitor, L-NAME, was added as a negative control. The reaction was stopped by adding stop buffer (400 μL) and then the equilibrated resin (100 μL) was added into each reaction mixture before the samples were transferred to spin cups. After centrifugation the eluates were counted in a liquid scintillation counter.

Animals, intracerebroventricular injections, and evaluation of antinociception

Male albino CD-1 mice weighing 22–25 g were housed and used strictly in accordance with the guidelines of the European Community for the Care and Use of Laboratory Animals (Council Directive 86/609/EEC). The experiments performed were previously approved by the Bioethics Committee of the "Consejo Superior de Investigaciones Científicas (CSIC)." The response of the animals to nociceptive stimuli and the influence of morphine sulfate (Merck) were determined using the warm water (52°C) tail-flick test using a cut-off time of 10 s to minimize the risk of tissue damage. Baseline latencies ranged from 1.5 to 2.0 s and they were not significantly affected by the inhibitors used: L-NG-Nitroarginine (LNNA, Tocris 0664; Biogen), Gö7874 (Calbiochem, #365252; VWR), Chelerythrine (Calbiochem #220285), MK801 (Tocris, #0924), D-AP5 (Tocris, #0106), KN93 (Calbiochem #422711), or their solvents. Antinociception is expressed as a percentage of the maximum possible effect (=100×[test latency-baseline latency]/[cut-off time-baseline latency]). Groups of 10 mice were lightly anesthetized with ether and received 10 nmol morphine sulfate (Merck) injected in a volume of 4 μL into the lateral ventricle. Thereafter, antinociception was assessed at different time intervals.

Previously characterized synthetic end-capped phosphorothioate (indicated as *) antisense ODN (synthesized by Sigma-Aldrich) were used to reduce the expression of the target RGSZ2 protein (NM_019958), generating RGSZ2-deficient mice (15) (Supplementary Fig. S3). The mouse KO with a targeted disruption of HINT1 (on a 129SvJ background) was generously supplied by I.B. Weinstein/J.B. Wang. Breeding pairs of homozygous WT and KO mice were obtained from hybrid mutant mice (originally generated on a 129SvJ-C57BL/6 background) by backcrossing 129SvJ mice for several generations. The genotype was confirmed by PCR analysis of DNA isolated from tail biopsies.

Acute tolerance and interval required to recover the analgesic response

The animals were icv-injected with 10 nmol morphine, a dose that produces 70%–80% of the maximum effect detected in this test, comparing the controls with the RGSZ2-deficient mice. Morphine antinociception was evaluated after 30 min when the peak effect of the compound was achieved. To study the recovery from acute analgesic tolerance and to avoid repeated injections of the mice, the animals were then divided into groups of eight mice each. Acute tolerance was determined in one of these groups by icv-injecting of a test dose of 10 nmol morphine 24 h after the priming dose. Afterward, additional doses of 10 nmol morphine were administered every 24 h but to a different group of mice. In RGSZ2-deficient mice, the recovery from acute tolerance was studied with and without concomitant ODN treatment. In all cases the mice were evaluated 30 min after morphine injection. Data are expressed as the mean ± standard error of the mean of groups of eight mice.

Immunocytochemistry

Deeply anaesthetized animals (Equithesin, Janssen Laboratories, 2.5 ml/kg intraperitoneally) were ventilated and perfused through the left ventricle with 0.9% saline, followed by 250 ml of a fixative solution containing 4% paraformaldehyde in 0.1 *M* phosphate buffer (pH 7.4). Brains were then removed, cut into small blocks, and postfixed for 4 h at room temperature in the same fixative. The blocks were then cryoprotected at 4°C in a 30% sucrose solution in phosphate buffer, and serial 40-μm-thick transverse frozen sections were obtained on a 2800 Frigocut (Reichert-Jung) microtome that were then processed for immunocytochemistry. The antibodies used in this study have already been characterized and they fulfill the recommended criteria for use in immunohistochemistry (41). All these antibodies were diluted in phosphate-buffered saline containing 0.2% Triton X-100. The expression of the nNOS protein was evaluated with a goat polyclonal antibody suitable for immunohistochemistry (Abcam ab1376). Endogenous RGSZ2 protein was identified with a rabbit polyclonal antibody that has been adequately characterized (15, 37). Immunofluorescence staining for confocal microscopy was carried out by incubating tissue sections overnight at 4°C with the primary antibodies against nNOS and RGSZ2 diluted 1:2500 and 1:500, respectively. After washing thoroughly in phosphate-buffered saline, antibody staining was observed with Alexa Fluor 488 donkey anti-goat IgG and Alexa Fluor 568 donkey anti-rabbit IgG (Molecular Probes), incubated for 1 h at room temperature. Confocal images were acquired on a Leica TCS SP5 scanner (Leica Microsystems GmbH). Controls for immunohistochemistry were performed following standard protocols (43).

Coimmunoprecipitation of signaling proteins

The PAGs were obtained from groups of eight mice at various intervals after icv injection of morphine, and synaptosomal membranes were obtained as described previously (12, 35). Briefly, the PAGs were collected and homogenized in a buffer containing 25 m*M* Tris-HCl (pH 7.4), 1 m*M* EGTA, and 0.32 *M* sucrose supplemented with a phosphatase and protease inhibitors. The homogenate was centrifuged at 1000 *g* for 10 min to remove the nuclear fraction, pellet 1 (P1), and the supernatant (S1) was centrifuged at 20,000 *g* for 20 min to obtain the crude synaptosomal pellet (P2) and the supernatant S2. The pellet P2 was diluted in Tris buffer supplemented with a mixture of protease inhibitors and added to the top layer of a

discontinuous step Percoll gradient (3%, 10%, 15%, and 23%). The tubes were centrifuged at 30,000 *g* at 4°C for 5 min and to diminish the presence of Percoll, the fraction containing the synaptosomes was diluted fourfold with ice-cold sucrose/EDTA buffer and centrifuged at 20,000 *g* for 30 min at 4°C. To obtain the synaptosomal membranes the pellet was placed in a hypotonic buffer and centrifuged at 20,000 *g* for 30 min at 4°C. The resulting pellet was then used in the subsequent experiments of MOR immunoprecipitation and analysis of coprecipitated proteins. To determine the possible internalization of the MOR as a consequence of morphine treatment, the supernatant (S2) was centrifuged at 105,000 *g* for 1 h to obtain the crude microsomal pellet (P3). The S3 supernatant was concentrated in Amicon Ultra-4 centrifugal filter devices (nominal molecular weight limit NMWL of 10,000 #UFC8 01024; Millipore Iberica S.A.), the proteins recovered were resolved by SDS-PAGE and the MORs analyzed in Western blots.

Antibodies against the second extracellular loop of the MOR and against the CT of RGSZ2 proteins were labeled with biotin (Pierce #21217 & 21339; Fisher Scientific). The target proteins were then immunoprecipitated from solubilized membranes and analyzed as described previously (34). Since unidentified proteins might coprecipitate with the MORs and interfere with the phosphoserine analysis (clone 1C8; Calbiochem, 525281), the existing protein interactions were disrupted under denaturing conditions before immunoprecipitation.

Detection of signaling proteins

Western blots were probed with affinity-purified IgG antibodies directed against peptide sequences in: the murine MOR, anti-MOR second extracellular loop, and anti-MOR CT (diluted 1:1000) (35); anti-RGS17(Z2) CT (aa: 192–215; GenScript), anti-RGS17(Z2) IQ (aa:46–60; GenScript) (15, 34), and anti-RGS17(Z2) W15 (sc-48286) internal region; anti-phospho-MOR (Ser375) (1:1000; Cell Signaling 3451; Izasa); anti-nNOS (1:1000; Santa Cruz sc1025; Quimigen); anti-phospho-nNOS (Ser847) (1 μg/ml; Abcam ab16650); anti-phospho-nNOS (Ser1417) (2 μg/ml; ab5583); anti-NMDAR1 (1:1000; ab1880); anti-phospho NMDAR1 (Ser890) (1:1000; Cell Signaling 3381); anti-NMDAR2A (1:1000, ab14596); anti-NMDAR2A phospho-Y1325 (1:300, ab16646); anti-Tyr416 phospho-nonreceptor tyrosine kinase (1:1000; Cell Signaling 2101); mouse monoclonal IgG1 anti-CaMKII (1:3000; BD Transduction labs, 611292; BD); anti-phospho-CaMKII (Thr286) (1:2000; Cell Signaling, 3361); anti-S-nitrosocysteine (1:1000; Abcam ab50185); anti-Actin (1:3000; Stressgen, CSA-400; Bionova). Other antibodies included a mouse monoclonal antibody (IgM) to detect clone 1C8 [goat anti-mouse IgM (Calbiochem, #401295) (H + L) conjugated to horseradish peroxidase. The antibodies were diluted in TBS + 0.05% Tween 20 (TTBS) and incubated with polyvinylidene fluoride membranes for 24 h at 6°C. The primary antibodies were detected using the corresponding secondary antibodies conjugated to horseradish peroxidase (diluted 1:10,000 in TTBS). Antibody binding was observed using ECL Plus Western Blotting Detection System (GE #RPN2132), and chemiluminescence was recorded with a ChemiImager IS-5500 (Alpha Innotech). The assays were typically performed twice or three times using samples obtained from independent groups of mice, and the results were consistent.

Statistical significance

Analysis of variance, followed by the Student-Newman-Keuls test (SigmaStat; SPSS Science Software), was performed and significance was defined as $p < 0.05$.

Acknowledgments

This research was supported by FIS PI080417 (P.S.B.), PS09/00332 (J.G.), and "Instituto de Salud Carlos III, Centro de Investigación Biomédica en Red de Salud Mental, CIBERSAM." M.R.M. is currently supported by a CIBERSAM contract, and A.V.S. is a predoctoral fellow from the Spanish Ministry of Science and Innovation. We would like to thank Beatriz Fraile and Gabriela de Alba for their excellent technical assistance.

Author Disclosure Statement

The authors declare that, excluding income received from our primary employer "Ministerio de Ciencia y Tecnología," no financial support or compensation has been received from any individual or corporate entity over the past 3 years for research or professional services and that there are no personal financial holdings that could be perceived as constituting a potential conflict of interest.

References

1. Ai W, Gong J, and Yu L. MAP kinase activation by mu opioid receptor involves phosphatidylinositol 3-kinase but not the cAMP/PKA pathway. *FEBS Lett* 456: 196–200, 1999.
2. Ajit SK, Ramineni S, Edris W, Hunt RA, Hum WT, Hepler JR, and Young KH. RGSZ1 interacts with protein kinase C interacting protein PKCI-1 and modulates mu opioid receptor signaling. *Cell Signal* 19: 723–730, 2007.
3. Bleakman D, Alt A, and Nisenbaum ES. Glutamate receptors and pain. *Semin Cell Dev Biol* 17: 592–604, 2006.
4. Braithwaite SP, Paul S, Nairn AC, and Lombroso PJ. Synaptic plasticity: one STEP at a time. *Trends Neurosci* 29: 452–458, 2006.
5. Brenman JE, Chao DS, Gee SH, McGee AW, Craven SE, Santillano DR, Wu Z, Huang F, Xia H, Peters MF, Froehner SC, and Bredt DS. Interaction of nitric oxide synthase with the postsynaptic density protein PSD-95 and alpha1-syntrophin mediated by PDZ domains. *Cell* 84: 757–767, 1996.
6. Brenner GJ, Ji RR, Shaffer S, and Woolf CJ. Peripheral noxious stimulation induces phosphorylation of the NMDA receptor NR1 subunit at the PKC-dependent site, serine-896, in spinal cord dorsal horn neurons. *Eur J Neurosci* 20: 375–384, 2004.
7. Chakrabarti S, Liu NJ, and Gintzler AR. Reciprocal modulation of phospholipase Cβ isoforms: adaptation to chronic morphine. *Proc Natl Acad Sci U S A* 100: 13686–13691, 2003.
8. Chen L and Huang LY. Sustained potentiation of NMDA receptor-mediated glutamate responses through activation of protein kinase C by a μ opioid. *Neuron* 7: 319–326, 1991.
9. Commons KG, van Bockstaele EJ, and Pfaff DW. Frequent colocalization of mu opioid and NMDA-type glutamate receptors at postsynaptic sites in periaqueductal gray neurons. *J Comp Neurol* 408: 549–559, 1999.
10. Daff S. NO synthase: structures and mechanisms. *Nitric Oxide* 23: 1–11, 2010.
11. Doyle GA, Furlong PJ, Schwebel CL, Smith GG, Lohoff FW, Buono RJ, Berrettini WH, and Ferraro TN. Fine mapping of a major QTL influencing morphine preference in C57BL/6 and DBA/2 mice using congenic strains. *Neuropsychopharmacology* 33: 2801–2809, 2008.

12. Dunkley PR, Jarvie PE, and Robinson PJ. A rapid Percoll gradient procedure for preparation of synaptosomes. *Nat Protoc* 3: 1718–1728, 2008.
13. Elliott K, Minami N, Kolesnikov YA, Pasternak GW, and Inturrisi CE. The NMDA receptor antagonists, LY274614 and MK-801, and the nitric oxide synthase inhibitor, NG-nitro-L-arginine, attenuate analgesic tolerance to the mu-opioid morphine but not to kappa opioids. *Pain* 56: 69–75, 1994.
14. Fisher K, Coderre TJ, and Hagen NA. Targeting the N-methyl-D-aspartate receptor for chronic pain management. Preclinical animal studies, recent clinical experience and future research directions. *J Pain Symptom Manage* 20: 358–373, 2000.
15. Garzón J, Rodríguez-Muñoz M, López-Fando A, and Sánchez-Blázquez P. The RGSZ2 protein exists in a complex with mu-opioid receptors and regulates the desensitizing capacity of Gz proteins. *Neuropsychopharmacology* 30: 1632–1648, 2005.
16. Garzón J, Rodríguez-Muñoz M, and Sánchez-Blázquez P. Do pharmacological approaches that prevent opioid tolerance target different elements in the same regulatory machinery? *Curr Drug Abuse Rev* 1: 222–238, 2008.
17. Glass MJ, Vanyo L, Quimson L, and Pickel VM. Ultrastructural relationship between N-methyl-D-aspartate-NR1 receptor subunit and mu-opioid receptor in the mouse central nucleus of the amygdala. *Neuroscience* 163: 857–867, 2009.
18. Guang W, Wang H, Su T, Weinstein IB, and Wang JB. Role of mPKCI, a novel mu-opioid receptor interactive protein, in receptor desensitization, phosphorylation, and morphine-induced analgesia. *Mol Pharmacol* 66: 1285–1292, 2004.
19. Heo J and Campbell SL. Ras regulation by reactive oxygen and nitrogen species. *Biochemistry* 45: 2200–2210, 2006.
20. Inoue M, Mishina M, and Ueda H. Locus-specific rescue of GluRε1 NMDA receptors in mutant mice identifies the brain regions important for morphine tolerance and dependence. *J Neurosci* 23: 6529–6536, 2003.
21. Kissin I, Bright CA, and Bradley EL Jr. The effect of ketamine on opioid-induced acute tolerance: can it explain reduction of opioid consumption with ketamine-opioid analgesic combinations? *Anesth Analg* 91: 1483–1488, 2000.
22. Kolesnikov Y, Jain S, Wilson R, and Pasternak GW. Lack of morphine and enkephalin tolerance in 129/SvEv mice: evidence for a NMDA receptor defect. *J Pharmacol Exp Ther* 284: 455–459, 1998.
23. Kow LM, Commons KG, Ogawa S, and Pfaff DW. Potentiation of the excitatory action of NMDA in ventrolateral periaqueductal gray by the mu-opioid receptor agonist, DAMGO. *Brain Res* 935: 87–102, 2002.
24. Koyama S and Akaike N. Activation of mu-opioid receptor selectively potentiates NMDA-induced outward currents in rat locus coeruleus neurons. *Neurosci Res* 60: 22–28, 2008.
25. Leak TS, Mychaleckyj JC, Smith SG, Keene KL, Gordon CJ, Hicks PJ, Freedman BI, Bowden DW, and Sale MM. Evaluation of a SNP map of 6q24-27 confirms diabetic nephropathy loci and identifies novel associations in type 2 diabetes patients with nephropathy from an African-American population. *Hum Genet* 124: 63–71, 2008.
26. Lu WY, Xiong ZG, Lei S, Orser BA, Dudek E, Browning MD, and MacDonald JF. G-protein-coupled receptors act via protein kinase C and Src to regulate NMDA receptors. *Nat Neurosci* 2: 331–338, 1999.
27. Luginbuhl M, Gerber A, Schnider TW, Petersen-Felix S, Arendt-Nielsen L, and Curatolo M. Modulation of remifentanil-induced analgesia, hyperalgesia, and tolerance by small-dose ketamine in humans. *Anesth Analg* 96: 726–732, 2003.
28. Mansour A, Khachaturian H, Lewis ME, Akil H, and Watson SJ. Anatomy of CNS opioid receptors. *Trends Neurosci* 11: 308–314, 1988.
29. Marek P, Ben-Eliyahu S, Vaccarino AL, and Liebeskind JC. Delayed application of MK-801 attenuates development of morphine tolerance in rats. *Brain Res* 558: 163–165, 1991.
30. Murthy KS and Makhlouf GM. Opioid mu, delta, and kappa receptor-induced activation of phospholipase C-beta 3 and inhibition of adenylyl cyclase is mediated by Gi2 and G(o) in smooth muscle. *Mol Pharmacol* 50: 870–877, 1996.
31. Narita M, Hashimoto K, Amano T, Narita M, Niikura K, Nakamura A, and Suzuki T. Post-synaptic action of morphine on glutamatergic neuronal transmission related to the descending antinociceptive pathway in the rat thalamus. *J Neurochem* 104: 469–478, 2008.
32. Pasternak GW, Kolesnikov YA, and Babey AM. Perspectives on the N-methyl-D-aspartate/nitric oxide cascade and opioid tolerance. *Neuropsychopharmacology* 13: 309–313, 1995.
33. Rameau GA, Tukey DS, Garcin-Hosfield ED, Titcombe RF, Misra C, Khatri L, Getzoff ED, and Ziff EB. Biphasic coupling of neuronal nitric oxide synthase phosphorylation to the NMDA receptor regulates AMPA receptor trafficking and neuronal cell death. *J Neurosci* 27: 3445–3455, 2007.
34. Rodríguez-Muñoz M, Bermúdez D, Sánchez-Blázquez P, and Garzón J. Sumoylated RGS-Rz proteins act as scaffolds for Mu-opioid receptors and G-protein complexes in mouse brain. *Neuropsychopharmacology* 32: 842–850, 2007.
35. Rodríguez-Muñoz M, de la Torre-Madrid E, Sánchez-Blázquez P, and Garzón J. Morphine induces endocytosis of neuronal mu-opioid receptors through the sustained transfer of Galpha subunits to RGSZ2 proteins. *Mol Pain* 3: 19, 2007.
36. Rodríguez-Muñoz M, de la Torre-Madrid E, Sánchez-Blázquez P, Wang JB, and Garzón J. NMDAR-nNOS generated zinc recruits PKCgamma to the HINT1-RGS17 complex bound to the C terminus of Mu-opioid receptors. *Cell Signal* 20: 1855–1864, 2008.
37. Rodríguez-Muñoz M, Sánchez-Blázquez P, Vicente-Sánchez A, Bailón C, Martín-Aznar B, and Garzón J. The histidine triad nucleotide-binding protein 1 supports mu-opioid receptor-glutamate NMDA receptor cross-regulation. *Cell Mol Life Sci* DOI 10.1007/s00018-010-0598-x, 2010.
38. Sánchez-Blázquez P, Rodríguez-Muñoz M, de la Torre-Madrid E, and Garzón J. Brain-specific Gαz interacts with Src tyrosine kinase to regulate Mu-opioid receptor-NMDAR signaling pathway. *Cell Signal* 21: 1444–1454, 2009.
39. Sánchez-Blázquez P, Rodríguez-Muñoz M, and Garzón J. Mu-opioid receptors transiently activate the Akt-nNOS pathway to produce sustained potentiation of PKC-mediated NMDAR-CaMKII signaling. *PLoS ONE* 5: e11278, 2010.
40. Sánchez-Blázquez P, Rodríguez-Muñoz M, Montero C, de la Torre-Madrid E, and Garzón J. Calcium/calmodulin-dependent protein kinase II supports morphine antinociceptive tolerance by phosphorylation of glycosylated phosducin-like protein. *Neuropharmacology* 54: 319–330, 2008.
41. Saper CB and Sawchenko PE. Magic peptides, magic antibodies: guidelines for appropriate controls for immunohistochemistry. *J Comp Neurol* 465: 161–163, 2003.
42. Schulz S, Mayer D, Pfeiffer M, Stumm R, Koch T, and Höllt V. Morphine induces terminal micro-opioid receptor desensitization by sustained phosphorylation of serine-375. *EMBO J* 23: 3282–3289, 2004.
43. Serrano J, Fernandez AP, Sánchez J, Rodrigo J, and Martínez A. Adrenomedullin expression is up-regulated by acute

hypobaric hypoxia in the cerebral cortex of the adult rat. *Brain Pathol* 18: 434–442, 2008.
44. Sierra DA, Gilbert DJ, Householder D, Grishin NV, Yu K, Ukidwe P, Barker SA, He W, Wensel TG, Otero G, Brown G, Copeland NG, Jenkins NA, and Wilkie TM. Evolution of the regulators of G-protein signaling multigene family in mouse and human. *Genomics* 79: 177–185, 2002.
45. Tochio H, Zhang Q, Mandal P, Li M, and Zhang M. Solution structure of the extended neuronal nitric oxide synthase PDZ domain complexed with an associated peptide. *Nat Struct Biol* 6: 417–421, 1999.
46. Trujillo KA and Akil H. Inhibition of morphine tolerance and dependence by the NMDA receptor antagonist MK-801. *Science* 251: 85–87, 1991.
47. Yaksh TL, Yeung JC, and Rudy TA. Systematic examination in the rat of brain sites sensitive to the direct application of morphine: observation of differential effects within the periaqueductal gray. *Brain Res* 114: 83–103, 1976.
48. Yun HY, Gonzalez-Zulueta M, Dawson VL, and Dawson TM. Nitric oxide mediates N-methyl-D-aspartate receptor-induced activation of p21ras. *Proc Natl Acad Sci U S A* 95: 5773–5778, 1998.
49. Zhou L and Zhu DY. Neuronal nitric oxide synthase: structure, subcellular localization, regulation, and clinical implications. *Nitric Oxide* 20: 223–230, 2009.
50. Zhu JJ, Qin Y, Zhao M, Van AL, and Malinow R. Ras and Rap control AMPA receptor trafficking during synaptic plasticity. *Cell* 110: 443–455, 2002.

Address correspondence to:
Dr. Pilar Sánchez-Blázquez
Cajal Institute
Consejo Superior de Investigaciones Científicas
Avd. Dr. Arce 37
Madrid 28002
Spain

E-mail: psb@cajal.csic.es

Date of first submission to ARS Central, November 8, 2010; date of final revised submission, February 24, 2011; date of acceptance, February 24, 2011.

Abbreviations Used

BiFC = bimolecular fluorescence complementation
CaMKII = calmodulin-dependent protein kinase II
CHO = Chinese hamster ovary
CRD = cysteine-rich domain
CT = C terminus
DAG = diacylglycerol
ELM = Eukaryotic Linear Motif
ERK = extracellular signal-regulated kinase
GPCR = G protein-coupled receptor
GST = glutathione S-transferase
HINT1 = histidine triad nucleotide binding protein 1
icv = intracerebroventricular
KO = knockout
MOR = Mu opioid receptor
NMDAR = *N*-methyl-D-aspartate receptor
nNOS = neural nitric oxide synthase
NO = nitric oxide
ODN = oligodeoxynucleotide
PAG = periaqueductal gray
PCR = polymerase chain reaction
PDZ = post synaptic density protein (PSD95), Drosophila disc large tumor suppressor (DlgA), and zonula occludens-1 protein (zo-1)
PI3K = phosphoinositide 3-kinase
PKC = protein kinase C
PSD-95 = postsynaptic density 95
RGS = regulator of G protein signaling
WT = wild type

This article has been cited by:

1. Pilar Sánchez-Blázquez , María Rodríguez-Muñoz , Concha Bailón , Javier Garzón . 2012. GPCRs Promote the Release of Zinc Ions Mediated by nNOS/NO and the Redox Transducer RGSZ2 Protein. *Antioxidants & Redox Signaling* **17**:9, 1163-1177. [Abstract] [Full Text HTML] [Full Text PDF] [Full Text PDF with Links] [Supplemental material]
2. Richard J. Bodnar. 2012. Endogenous Opiates and Behavior: 2011. *Peptides* . [CrossRef]
3. María Rodríguez-Muñoz, Pilar Sánchez-Blázquez, Ana Vicente-Sánchez, Esther Berrocoso, Javier Garzón. 2011. The Mu-Opioid Receptor and the NMDA Receptor Associate in PAG Neurons: Implications in Pain Control. *Neuropsychopharmacology* . [CrossRef]